Chapter

IPMC Based Flexible Platform: A Boon to the Alternative Energy Solution

Monojit Mondal, Arkaprava Datta and Tarun Kanti Bhattacharyya

Abstract

The ameliorating urge for energy in consonance with the descending environment and attenuation of natural resources leads to the development of alternate energy storage. Realistically, flexible, portable, and lightweight energy storage devices have immense popularity for accessible transportation. In this context, this chapter analyses a possible solution to the problems described aforesaid on IPMC (Ionic Polymer Metal Composite) membranes. Also, this chapter includes porosity induced electrolyte polymer membrane by MCP of Nafion enhances electrical harvesting attribution. The novel and transportable ocean kinetic energy converting platform by IPMC membrane was fabricated and applied for energy conversion. The etching and surface sanding advances the surface area of IPMC to escalate the gas generation rate as an electrolyser. The functionalised infiltrated Nafion nanocomposite membranes are fabricated and analysed for DMFC performance and methanol permeability. Perfluorosulfonic acid polymer electrolyte membranes gained more attention in the former epoch for vast applications in energy, chloro-alkali electrolytes, OER, and polymer electrolyte fuel cells. The direct methanol fuel cell is an excellent alternative to PEFC for managing liquid fuel and higher energy density at low operational temperatures. Nevertheless, polymer electrolyte membranes and direct methanol fuel cells are potential contenders for circulated power and transferable power applications; the substantial technical, scientific, and economic difficulties must be elucidated beforehand commercialisation.

Keywords: Energy storage, Fuel cell, IPMC, Flexible storage, smart material, ionic polymer, electro-active polymer, Composite membrane, Electrochemistry

1. Introduction

Over the century, the evolution of electronic devices has been rehabilitated rapidly and day by day. The transistor incorporation led to reducing the feature size of any realistic instruments, and besides that, the efficacy has to be ameliorated for that purpose. The continual advancement of the fabrication methodologies of printed circuit boards makes the transistors significantly small, permitting the huge number of transistors in one plate and lessen the consumption of electric power of the integrated circuit. In the present day, many electronic devices are used in miniature sizes and too much power for any operation. Subsequently, energy

storage devices are required in the same formation used in those new small devices, batteries, and capacitors, which are hindrances to their improvement. The batteries are analysed, which are lower of flexibility, higher weight, and mainly possess huge space in the particular equipment. Generally, the capacitors with low storage capacity with low energy occupy a huge space, mainly electrolytic capacitors, restrained by shape. Moreover, the capacitors need to solder directly to the integrated circuit; their electrical polarity cannot be reversed in electrolytic capacitors. In this scenario, this chapter explores a probable elucidation to the above-said context based on IPMC (ionic polymer-metal composite) systems. These attain capacitive features after dipping in the ionic solution; then, the membrane becomes flexible and lightweight with stored potential, a new kind of flexible capacitor. Furthermore, the flexible IPMC membrane capacitor is malleable and easily used in polarity reversal based on needs. In most cases, the analysis and application of the IPMC polymer matrix entirely focused on the actuator's application [1–5]. This chapter focused on another part of IPMC, i.e., the energy storage application. The different fabrication procedures and corresponding attributes of the polymer system are discussed thoroughly here. Prominent displacements analyse IPMCs within lower density forces. In the mechanical energy harvesting system, IPMCs are investigated using the generated lower electric power values, but irrespective of using significant mechanical pressures, the reverse function is happened as with the piezoelectric type materials [6, 7]. Present-day, electric double-layer capacitors (EDLCs) and lithium-ion batteries are the maxima used energy storage devices on the scale of important commercial use. Every device exhibits definite attribution and applications that need high energy density ($Whkg^{-1}$) for lithium batteries and high power density (Wkg^{-1}) of EDLC system [8–11]. Furthermore, few polymers depict several characteristics changes and some benefits in the potential application field in the presence of electrical stimulation; those are called electro-active polymers or EAPs. Those materials are showing response in size and shape by the variation of electrical stimulation. This material is categorised into two depending on the activation mechanism, i.e., ionic and electronic or field-activated [12, 13]. Generally, the electronic grade exhibits a higher energy density of mechanical energy; in comparison, ionic systems potentially employed ion diffusion or transportation consist of the electrolyte-electrode interface. Conductive polymers, ionic polymer gels, and composites of ionic polymer-metal are examples of some ionic EAPs. The electromechanical response of the membrane, showing huge strain at electrical stimulation, is very similar to the biological tissues. The Ionic polymers are introduced in fuel cells application in the 1960s; the features of EAP and the connexion of electromechanical ion-transportation of metal-ionic polymer composites (IPMC) were invented in 1992 by researchers in the United States and Japan [14, 15]. In general, IPMC comprises a membrane of polyelectrolyte, normally Flemion or Nafion covered on all sides with a conductive metal. After that, the counter-ions are neutralised, stabilising the electrical anionic charge of the covalently stable to the pillar of the membrane. The hydrated cations transportation between an IPMC polymer matrix is kept within the voltage applied, and corresponding electrostatic interactions enhance the bending. IPMCs are the working actuator that delineates lower impedance. Moreover, the water-based IPMCs generally dissociate with solvent content when it is subjected to 1.23 Volts higher. IPMCs are corroborated as the smartest prominence materials for larger bending deformation and lighter weight within significantly less applied voltages [16–18]. However, To fabricate chemically coated IPMC membrane, electrodes of metal ions gold, platinum, etc., are distributed through the hydrophilic sections of the polymer matrix and generally decrease the consistent metal atoms of zero-valence. Paddison et al. [19] researched the measurement of hydrated Nafion's permittivity in the

range of broadband frequency. Their outcomes denote that the dielectric constant enhances with incrementing the water content, reduced with frequency increase.

2. Different manufacturing process of IPMC membrane

The important pillar for IPMC manufacture procedure is choosing the base ion altercation polymers; those are naturally fabricated from the organic polymers, comprising a permanent ionic group of covalently bonded. In the electrochemical industry, generally well-known ion exchange materials are used that rely on a copolymer of divinylbenzene and styrene. Moreover, the permanent ionic groups are shaped after the completion of polymerisation. The widely held ion altercation materials are alkene of perfluorinated: with lesser length side-chains concluded by ionic groups like Nafion, normally ammonium cations for anion exchange or carboxylate or sulfonate (COO^- or SO^{3-}) for exchange of cations. In a perfluorinated compound (PFC), all hydrogen is supplanted by fluorine in the chain of carbon; however, the molecule holds one altered functional group or atom at least. The backbones of large polymer conclude their short side-chains and mechanical strength afford ionic groups that interrelate with water and the transportation of suitable ions. Furthermore, they might generate nano-channels of hydrophilic nature that are called cluster networks. Yu. et al. was fabricated the IPMC polymer matrix using the as follows method. However, in this process, the perfluorinated ion exchange membrane is taken upon that metal is deposited, such as platinum or gold. The IPMC matrix samplings were constructed with the twice depositing of platinum on Nafion–117 [20]. The initial stage is to coarsen the material surface; a) the emery paper is used to scratch the membrane surface for increasing the effective surface area; b) using an ultrasonic cleaner, the membrane is cleaned with preferable water; c) the membrane is dipped and boiled the in aqueous hydrochloric acid, i.e., HCl aqueous of 2 N concentration for 30 minutes to eradicate the ions and impurities in the membrane, d) finally after the rinsing with DI water, the entire membrane is merged in hot deionised (DI) water for up to 30 minutes to eliminate acid and swelling the polymer membrane matrix. The coarsened membrane is kept in deionised water. The subsequent procedure steps are to integrate the ion transportation or altercation capability with the help of a complex metal solution. The platinum amine complex ($[Pt(NH_3)_4]Cl_2$) aqueous solution is used. Furthermore, when the polymer membrane is submerged, a solution of ammonium hydroxide (5%,1 ml) is added that to neutralise. Store the membrane at room temperature in the solution for more than three hours. Following Yu et al., the third step is primary plating. In this procedure, the complex of platinum cations is decreased to a metallic state as nano-particles form with the help of a prominence-reducing agent. After the rinsed in 180 ml 40°C deionised water, sodium borohydride (2 ml of 5%) is mixed in each 30 min for seven times. Within this arrangement, the temperature is raised progressively to 60°C for 1.5 hours. A smooth Pt particles black layer is coated in the membrane surface. After that, the entire polymer matrix, i.e., the membrane, is again washed with deionised (DI) water and plunge in 0.1 N dilute hydrochloric acid for up to one hour. In the finishing procedure, the secondary layer of plating is completed. This methodology is envisioned to deposit Pt over top of the preliminary surface of Pt to diminish the resistance of the surface. Next, the supplementary quantity of Pt is overlaid with the following methods into the as grow Pt layer. Furthermore, hydroxylamine (6 ml) and 5% hydrochloride solution are added, and 20% of hydrazine solution (3 ml) is mixed in every single 30 minutes interval simultaneously. In this sequential fabrication route, the temperature is elevated to 60°C progressively for four hours; after that, the grey metallic texture

will be coated on the membrane surface. After that, when no platinum ions are there in the solution of plating, the membrane is adequately washed with water and again placed in boiling in 0.1 N hydrochloric acid (dilute) to eliminate the cations of ammonium of the membrane.

2.1 Casting method and silica gel process

The economically available Nafion film thickness varies in the range of $50 \sim 180$ μm, though the efficiency of the IPMC differs by thickness, like the rigidity of bending, a field of electric, etc. However, to attain a denser or targeted depth of Nafion membrane irrespective of customised thickness, the entire process is illustrated below. Furthermore, this procedure needs a very controlled tuning of the method's parameters like the specific solvent concentration and temperature; therefore, it has reproductivity issues [21]. The thickness of Nafion may be attuned by the fine-tuning of volume dispersion of the Nafion. The overall fabrication procedure comprises four steps (a) stirring, (b) mixing and (c) thermal treatment, and (d) sonication. Thermal handling enhances the Nafion film's mechanical stiffness. Lastly, the Nafion film must be placed in the hydrogen peroxide solution in boiling state for 1 hour within temperature range 75°C -100°C and then the membrane heated for 1 hour in the deionised (DI) water. Furthermore, the process of casting has been testified to attain higher thickness Nafion IPMC actuators [22]. Moreover, Jung et al. was established a Nafion membrane of controlled pore size with porosity by silica sol–gel methods and etching by hydrofluoric acid [23]. Furthermore, they established an improved metal composite actuator consisting of ionic polymer with the help of Nafion membrane having porosity using the ion exchange procedure and electroless plating. After that, (i) the different Nafion surface possessing membranes were coarsened with sandpaper #1200 grading, and after that, the surface is substantially cleaned by ultrasonication cleaning method and chemically using HCl solution (2.5 N); (ii) for the exchange methods of Pt ion, the membranes were dipped in $[Pt(NH_3)_4]Cl_2.xH_2O$ solution (0.2 wt%), and then ultrasonicated for 8 h with 30 min interval; (iii) for the initial reduction methods, an aqueous solution about 180 ml having NH4OH (0.5 ml) solution was arranged, and then the membranes are absorbed in that solution; (iv) 1 wt% (0.5 ml) PVP solution and 2 mL of 5 wt% $NaBH_4$ solution is mixed in each 10 min interval; and (v) while the temperature of the solution is 600°C, the 20 mL of $NaBH_4$ solution (5 wt%) was mixed, and after that PVP solution (0.5 ml 1 wt%) was mixed at intervals of 20 min for four times. Finally, while this method was concluded, the membranes were dipped for 12 h in 0.1 N HCl solutions and then cleaned with deionised (DI) water. Thus, the membranes were accomplished by the Pt ion exchange methods of four cycles and the methods of initial reduction. Also, in the second-reduction methods, an aqueous solution of 280 mL is made that contains $[Pt(NH_3)_4]Cl_2.xH_2O$ (400 mg) was executed, and the membrane was dipped in that solution at 400C. Then 3 mL of NH2OH-HCl solution (5 wt%) and 6 mL of $NH_2NH_2.H_2O$ solution (20 wt%) were mixed with each 10 min. After that, the membrane was cleaned with DI water and 0.1 N HCl solutions. Lastly, in cation exchange, the membranes were dipped for 48 h in 1.5 N LiCl solutions (**Figure 1**).

2.2 Nafion-CNT composite based IPMC membrane

Ijeri et al. have prepared a carbon nanotube and Nafion polymer nanocomposite for combinational electron and proton transportation. The membranes depict the proficiency to permit a separate electron-proton transportation path inside the
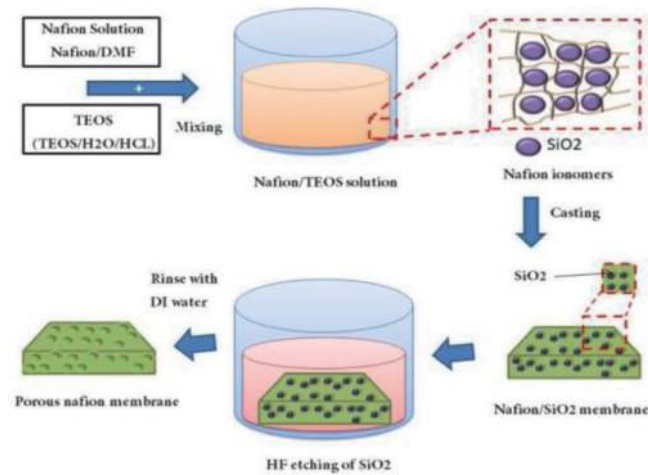
Figure 1.
Schematic representation of the fabrication of Nafion membrane technology incorporated with porosity [23].

membrane matrix. This feature unfastens new applications in particular membranes like advanced synthetic devices proficient in working sunlight to harvest hydrogen using water splitting. The manufacturing procedure is delineated as follows [24]. First, the needed amounts of MWCNTs and Nafion solution were weighed and put for 20 min in an ultrasonic cleaning bath with water. This provided a uniform dispersal of MWCNTs. The quantities were designed to provide MWCNT (0–5%) on a dry weight basis in nafion. In addition, isopropyl alcohol (1 ml) was mixed to assist in the proper dispersion and wetting of MWCNTs. Whenever the homogenous solution was decanted into petri dishes, it was kept on a furnace, maintaining that it is placed in an equal height levelled flat platform allowing uniform evaporation of solvent for 3 h within ambient conditions. Moreover, the entire setup was then replaced at 40°C and in the oven overnight. Furthermore, the membrane was then moistened with deionised (DI) water for one hour, separating the membrane from the entire setup substrate. Finally, self-supporting, flexible membranes were fabricated by just detaching them from the entire petri dish. Finally, the membrane was dried again and kept in an oven overnight.

2.3 Fabrication procedure by silver nanolayer in the membrane

Chung et al. introduce nanopowder of silver for IPMC fabrication membrane, which progresses the adhesion between polymer membrane matrix and metal electrode [25]. The normal methodologies of this process are the nanopowders of silver casting with Nafion polymer trailed by ornamentation and technologies of electroless plating of silver. The IPMC actuator of 5 mm (width) x 2 cm (length) x 0.23 mm (thickness) is taken for deformation investigation. The IPMC membrane corroborates a huge bending deformation with more than 90^0 angle curvature bending at 3 V applied. For the Ag nanopowder casting, the in-between adhesion of the electrode of metal and the polymer matrix membrane delineates superior attributes; however, this will enhance the surface resistance up to 2 Ω/square. To solve these difficulties, a non-toxic electroless plating of silver is introduced to diminish the resistance of the surface. Moreover, the resistance of the surface is lessened to 0.12–0.15 Ω/square after this electroless plating method. Furthermore, in the procedure, the contact pad will incline to form Ag_2O for the oxidation of Ag by the influence of OH^- from the water that will increment more the resistance of the

surface. The nickel electroforming in the contact pad will lessen the surface's resistance because it will preclude the Ag_2O formation. This novel is emerging procedure has the eminence of the better bond between the polymer membrane and electrode, shorter process time, substantial driving force in the lower driving voltage (around 0.22gf at 3 V), low cost those making it potential for application of mems based device (**Figure 2**).

2.4 The process of hot-pressing

The hot-pressing method is used to fabricate numerous thin films of Nafion observe together, which improves the stiffness of bending, reproducibility, and force performance. The key benefits of this process are that it is simple, repeatable, and lucid to regulate the thickness [26]. Mainly the actuators of IPMC are fabricated by this method. Modify the films of Nafion with appropriate dimensions, clean by the acetone, and pile by the polyimide film in the mildew. The mould setup is then positioned between the 180°C preheated setup with presses for 20 minutes without
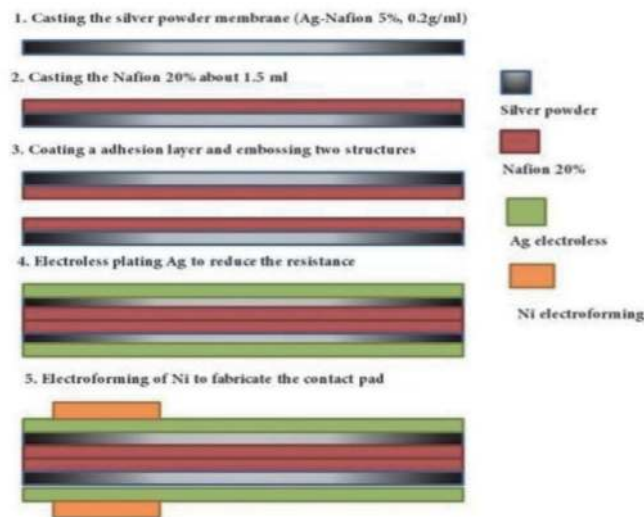

Figure 2.
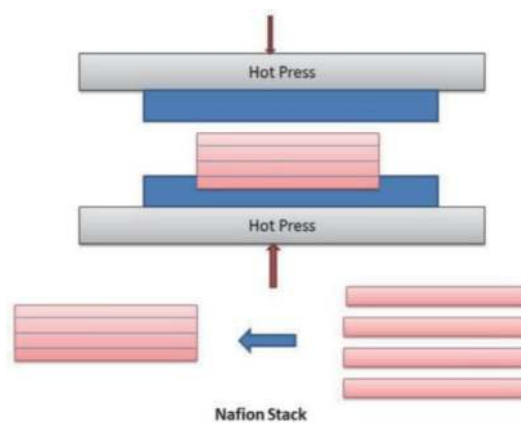*The schematic method flow of Ag nano-powders coated IPMC actuator [25].*

Figure 3.
Fabrication by hot press and stacking [27].

pressure, and at 180°C, then it is hard-pressed in the pressure of 50 MPa up to 10 min. After the films are cooled in ambient air to ambient temperature, the film is boiled for 1 hour at 70°C 3 wt% sulphuric acids for 1 hour at 70°C in 10 wt% hydrogen peroxide for 0.5 hours in DI water. Furthermore, dipped in platinum ammine complex ($[Pt(NH_3)_4Cl_2]$) aqueous solution for one to two days for platinum ions absorption in the piled film. Furthermore, after cleaning the membrane with deionised (DI) water, keeping it at 40°C water of 500 ml, stirring and mixed sodium borohydride (5 wt%, 5 ml) solution in 30 min every interval and also temperature steadily incremented up to 60°C (**Figure 3**).

3. Properties of IPMC

3.1 Actuation of IPMC membrane

When a membrane of Nafion-based IPMC polymer is induced to a slight amount of DC potential, the membrane experiences a deformation of rapid bending incline to the anode, trailed by a time-taking relaxation headed for cathode that is in the opposite direction. When both surfaces are connected after the movement of relaxation has clogged, the test sample exhibits a faster deformation of bending in the direction of cathode and, after that, gradually relaxes to its prior position to the anode direction.

3.2 Electrical and mechanical features of IPMC

It is established that the IPMC holds high modulus of elasticity and stiffness than the Nafion membrane, while both trails a similar pattern from the stress and strain analysis. This is because strain–stress performance is prevailed by the polymer than the powers of metal (as coated as electrode material). At the time, IPMC functions in a mode of bending; there is dissimilarity in mechanical features of the particles of metal (in the electrode) and network of polymer likely to influence one another. Moreover, fabricating a potential strain and stress plot of the IPMC membrane should be tested and cut as a cantilever configuration. The impedance analysis is delineated that IPMC works as an impartially capacitive material in low-frequency (>100 μF) and a resistive material like >50 Ω in higher frequency (**Figure 4**) [26].
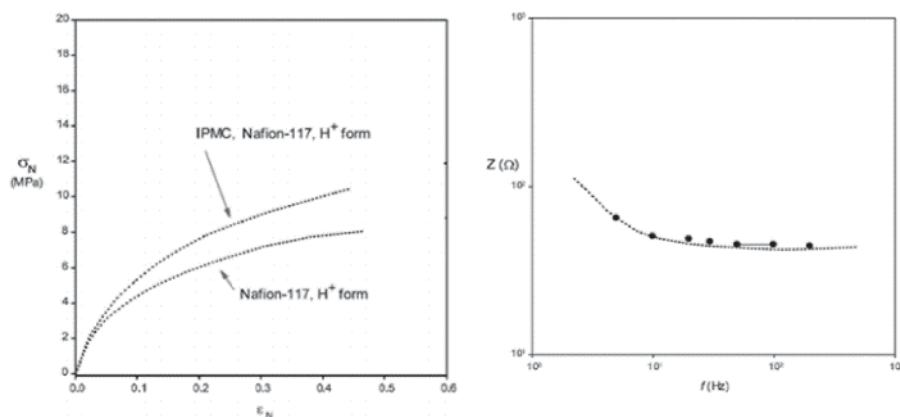

Figure 4.
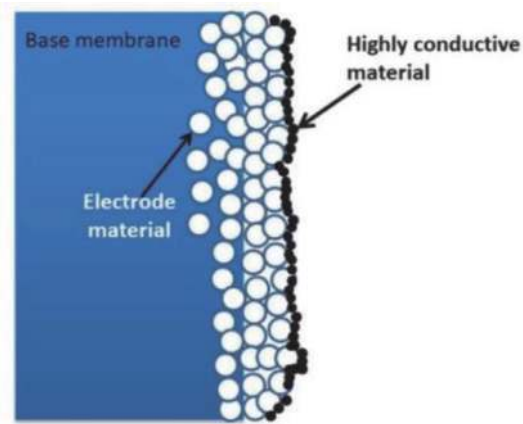*Impedance spectra of wet IPMC sample at fully hydrated state [27].*

Figure 5.
Schematic representation of the deposition process of higher conductive material [27].

3.3 Effect of cations variation

Kim and Shahinpoor [28] investigated in detail to realise that IPMC polymer matrix features vary depending on cations variation. Each membrane was manufactured to absorb dissimilar counter-ions likely as Li^+, Na^+, H^+, Ca^{2+}, K^+, Ba^{2+}, Mg^{2+} by sopping it in a particular solution of salt (1.5 N of LiCl, NaCl, HCl, CaCl$_2$, KCL, BaCl$_2$, MgCl$_2$), individually for 3 days at 30°C [6, 29, 30]. All the IPMC sample is monitored at null displacement holding different cations with respect to the Na^+ ions in IPMC. So it is clear that Li^+ — comprising IPMC is more outstanding than others, representing those hydration procedures compared to transportable cations that create a prominent character in actuation. Similarly, Flemion corroborates the same response (**Figure 5**) [31].

3.4 Lowering of IPMC electrode surface resistance

The resistance of the surface shows a crucial part in the electro-deformation of IPMC. Shahinpoor and Kim [32] abridge the resistance of active electrode surface effects on the prominence of artificial IPMC system is inclusive [33, 34]. It is observed under the scanning electron microscope (SEM), the surface cracks on the IPMC are easily visible, and pores are easily distinguishable. The relaxation and contraction are repeatedly shown when actuation bending of an IPMC generates more electrode surface cracks and depreciates the IPMC conductivity of the surface. If the IPMC electrode surface has a high resistance surface, the solvent molecules and cations membrane inside will transport to the outer side electrodes associated with the supply of power for the gradient encouraged in the field of electricity. The AC impedance analysis is an electrochemical method that helps to investigate IPMC artificial systems that elucidate the structure's equivalent circuit. The surface-electrode resistances (Rss), the polymer resistance (Rp), and impedance (Zw) for the charge transportation resistance nearby the surface electrode, with the double layer capacitance, relates in the interface of electrode-surface-electrolyte (Cd) and ionic polymer. In general, the surface electrode length (L) and the thickness of the surface electrode (t) play an essential role [27].

4. Energy storage study of IPMC polymer system

The electro-active IPMC material comprises a central layer possessed by a polymer with the upper and lower layer prepared of higher conductive electrodes.

The polymer that conquers the central layer has two main attributes: ion selectivity and permeability. These features are accomplished using polymers comprising organic ionic groups involved by covalent bonds to the polymer's backbone. Rely on the sign of the charge of the ionic groups existing in the polymer; it may be penetrable to cationic charge, i.e., positive and anionic charge, i.e., negative, or both. The polymers are commonly used with fixed ionic sulfonate groups for permeable positive ionic charges [35]. Furthermore, it is stated that one of the most standard groups of polymers worked in IPMC is "perfluorinated alkene," and specimens of these polymers are Nafion, Neoseptat, Flemiont or Selemiont, and Aciplext [35]. The electrodes founding the upper and lower layers of IPMCs are electrical conductors, investigated by very low electric resistivity. They are generally platinum (Pt) or silver (Ag) [36]. In the methods of fabrication of an IPMC, the electrodes deposition is presently made on the upper and lower active surfaces in three techniques: the route of "incorporation through reduction" (suffusing reduction methods) [29]; the physical casting procedure and the "direct mounting methods" (natural process assembly). The latter was established to elucidate the main difficulty of the two other manufacturing methods: the poor control in the deposition time of electrodes. The efficacy of the "integration through reduction" methodologies has created this the most worked, despite being the most time-taking and highly expensive [37]. IPMC membranes were fabricated using Nafion 117 polymer that is penetrable to positive ionic charges. The electrodes were deposited by high conducting metal like platinum or gold on the polymer using the "integration by reduction" procedures. Moreover, the disadvantage of holding poor control in the surface features of the electrodes typically reasons IPMC membranes to have different textures. The surface morphology and geometry of the electrodes of the IPMCs must be associated with their enactment, concomitant with the electrodes' electric resistance, and the consequential IPMC dielectric constant. Fundamentally, existing research work uses IPMC materials as actuation elements in electromechanical systems [30, 38–42]. A research was conducted on the capabilities of electro-active IPMC capacitors and the requirement of these possibilities on temperature [43–47]. Numerous IPMC membranes were observed with the same thickness but varying active surface areas. The membranes did not need any electrolyte that is why it is called "dry" strips with those capacitor elements. The polymer constituent of the membranes was acquired from a sheet of Nafion 117 and having a definite thickness. After cutting, a layer of chromium of 5 nm thickness was coated on the polymer surface, followed by a gold layer with a thickness of 100 nm on that same platform. Chromium was used to guarantee good adhesion between the gold and the polymeric matrix. The features of the voltage terminals of the composite material were chronicled within charge and discharge tests. All assays were done when charging the IPMC using a current power source, from which constant current charge was produced. Each IPMC was charged over fixed time using a fixed electric charging current in mA and then allowed to discharge, investigating the material property itself, i.e., how long they hold a charge. Moreover, the obtained results are calculated, and the exhibited capacitance value of specific and areal both have in the very higher range. The charging procedure is happened very fast up to the limit. The operating voltage was also perceived that the operating voltage is set up to that above which the IPMC got disrupted. Some of the used IPMC membranes were cut to test their storage capacitance scalability with their effective surface area. It was witnessed that a lessening of 20% of the surface area amounted to a reduction of 20% of its storage capacitance, such as a linear relationship [48]. Another research work verified a system for producing and storing electrical energy using IPMC devices and polymeric polyvinylidene difluoride (PVDF) piezoelectric devices to feed emitting organic diodes. For the electrical energy storage of IPMC, electro-active devices were worked, also for the production of electrical energy, PVDF piezoelectric elements

were employed, both as-fabricated single and double layers. The feasibility of IPMCs as electric energy storage elements was measured. The experiments were executed concerning the duration of the electrical charge store in the IPMC and reached the voltage level when the charging mechanism occurred at a constant voltage and constant current. Mainly The Nafion polymer is used in the IPMCs. The chromium electrodes were worked with an intermediary layer between the gold and the polymeric matrix, and also, the electrical contact from the gold platform is easy to make up [49, 50]. The storage capability of the IPMC membranes was certified with the integration of lithium ions in their interior structure. This for the initial doping of the IPMCs matrix was executed by dipping the devices in LiCl solution. The fabricated morphology of IPMCs matrix and metal-doped IPMC membranes stored charge in the greatest amount within a particular time window compared to the other storage elements, especially electrolytic capacitors, which exhibited specific and areal capacitances, too high. This work allows us to determine the relatively short electric charge of this material (**Figure 6**).

4.1 Electric model representing IPMCs as electrical energy storage elements

Dependent on the IPMC element mode, a variation of its theoretical model had to be prepared. This section analyses the various aspects and effects of the entire force on the positive ionic charges when the IPMC stores electrical energy. Electrical forces: When a continual electric current is enforced on the IPMC matrix, this leads to the positive ions, which are primarily at rest within the negative ionic polymer charges, to transport in the direction of one electrode. However, the negative ionic costs in the polymer are permanent; they will not be transportable. The gap between the positive and negative ionic charges will then escalate to the genesis of an electric field inside the IPMC matrix; there is a potential difference in its terminals and electrical forces between the IPMC systems. Mass diffusion forces: Mass diffusion forces are important in the experimental stage. When an IPMC membrane is dipped in an electrolyte, the forces for the mass diffusion method contribute to the impregnation of the membrane with the component positive ionic charges of the electrolyte. At the time of positive ionic charges, concentration in the membrane equals outside positive ionic charges. The concentration on the outer surface is residual; a substantial concentration gradient can transfer charges into the polymer matrix. Nafion 117's polymer encompasses negative charges, making the IPMC membrane selective only to positive charges concerned by the electrical forces
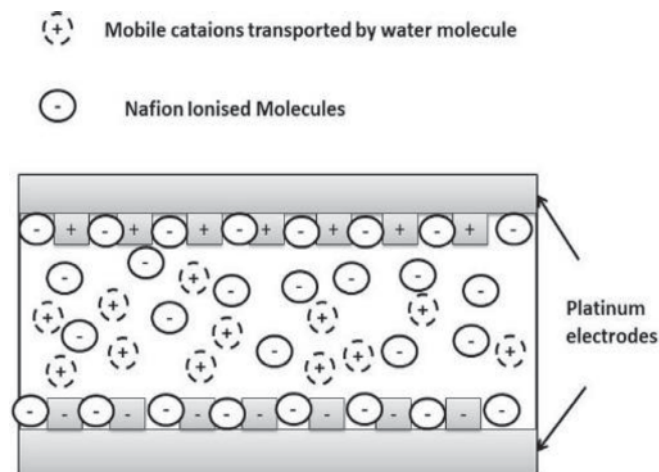

Figure 6.
Illustration of ionic distribution in the IPMC based system [51].

between them and the negative fixed charges. Mechanical forces: There are no mechanical pressures forced on the IPMC capacitor. The positive ionic charges current density: regarding the forces' characterisation, one arrives at Eq. (1) for the positive ionic charges current density within the IPMC.

$$J_+ \approx -\left(\frac{RT}{K}\right)\nabla^+_{\rho c} - \left(\frac{q+}{kp}\right)\nabla_{pmec} \qquad (1)$$

4.2 Discharging and charging of IPMCs at constant current

The discharge investigation under a resistive load intended to acquire the specific capacitance values C_{eq} (Fg^{-1}) connected with a specific IPMC membrane, i.e., a capacitive element, and compute each discharge time t_d and each used electrolyte. To execute a discharge test, it is essential to execute the electrical charging of each IPMC capacitive membrane. However, in every discharge, the test contained two divergent phases: discharging through a resistor and constant voltage charging. The obtained value was selected to have a much low value than the internal IPMC R_{dif} resistance. This is expected to realise the synchronised use of two membranes of IPMC materials connected in parallel. The upper IPMC electrodes were associated with the positive terminal of the external DC voltage, while the lower electrodes were coupled to its negative terminal. There is a discharge resistance, i.e., R_{ext} is present in between the terminals of the external circuit. Two of the most significant parameters for analysing a device for electrical energy storage are the rated voltage V_n and charging time t_s. A series of IPMC charge tests are executed at a constant current to acquire values for those two parameters. The current source has the main benefits of being consistent for quite lower values of current in the mA order, and the voltage is controlled. The usage of the lower current value is for charging the IPMC is vindicated by these for being usable in low-power devices. This voltage source permits the constant current imposition to the IPMC capacitive membrane elements is crucial for the investigations of charging and discharging. The net gain in the current power source is better. The IPMC charging analyses were carried out at a constant current. This value was selected because the thinnest IPMC used in those tests reaches its nominal voltage of 1.5 V.

4.3 Duty cycle

The quantity of charge–discharge cycles provides the valuable life of a precise electrical energy storage device that can tolerate ago no longer being fit for operation. Those parameters are essential for indicating how long or for how many cycles the elements can be worked for a specific application. To conclude whether altered solute concentrations could enhance the useful life of an IPMC capacitive membrane, numerous consecutive charging and discharging investigation at constant current were executed. This harvests a square waveform of electric current conforming to charging and discharging cycles at fixed current. The waveform was asymmetric because a negative current in the discharge time was introduced, and the IPMC terminal voltage would reach negative values [51].

4.4 Holding time

Preferably, a device for electrical energy storing should deliver all of the electrical energy previously-stored irrespective of the time at which it was stored. The IPMC electromechanical model delineates that the electric charge in the IPMC system is related to the terminals voltage in Eq. (2). This designates that the electric

charge stored in an IPMC is directly proportional to the voltage between its terminals, as in a capacitor.

$$Q = \frac{3\varepsilon bl}{5d} V \qquad (2)$$

The experimental methods for assessing the conservation of electrical charge in IPMC capacitive elements had two dissimilar parts; whole charging of the IPMC following the analysis of its voltage at subsequent instants of time [52]. When the IPMC rated voltage is reached, the current source was turned off. The terminals voltages of the membrane were then calculated by varying times. The IPMC material depicts capacitive behaviour, and the value of its capacitance relies on the dielectric constant as in Eq. (3).

$$C_{eq} = \frac{3\varepsilon bl}{5d} \qquad (3)$$

The specific capacitance C_{eq_e} (F kg^{-1}) of a given IPMC membrane is measured by Eq. (4), where r is the equivalent mass density of the IPMC membrane.

$$Ceq\_e = \frac{Ceq}{m} = \left(\frac{3\varepsilon bl}{5d}\right) \cdot \frac{1}{(\rho.b.l.d)} = \frac{3\varepsilon}{\rho d^2} \qquad (4)$$

The dielectric constant value of the as-fabricated IPMC capacitive system is affected by the electrolyte used and the negative ionic charge density of existing connections to the polymeric morphology. Therefore, the connexion between the dielectric constants of two different IPMC membranes, if assembled in the same electrolyte, is only depicted by the ratio existing within the negative ionic charges density in the same element, which in turn will rely on the volume of the IPMC system ($b.l.d$) and the ionic charges density of the polymeric matrix used, k, stated by the following relation in Eq. (5).

$$\varepsilon \propto k.b.l.d \qquad (5)$$

The significant time evolution of the voltage at resistance R_{ext} throughout the IPMC discharge is given by Eq. (6), where U is the voltage at the preliminary instant, R_{ext} is the electrical discharge resistance, and Ceq is the equivalent capacitance of the IPMC element.

$$\vartheta(t) = U.e^{-\frac{t}{R_{ext}.Ceq}} \qquad (6)$$

The primary technique contained the numerical approximation of the voltage curves acquired experimentally via Eq. (6). The methodologies of nonlinear least squares with the help of the confidence region algorithm were introduced to assess C_{eq}. The R_{ext} had a value in the range kΩ. As the regression curve calculated was not a better approximation of the experimental data curve. Eq. (6) for the capacitance of IPMC equivalent presumes only a single capacitive effect in IPMC membranes. This is delineated for the transportation of positive ionic charges in between the polymer matrix, and it's accumulated along the whole surface of the electrode with a negative polarity (**Figure** 7).

Moreover, when the low-frequency is applied electrical signals like 0.1 Hz in this proportion of electro-active material, the positive ionic charges circulated the inner side of the IPMC matrix quickly gathered the nearby zone of the negative electrode, and consecutively the capacitive double layer is formed. The outcomes of
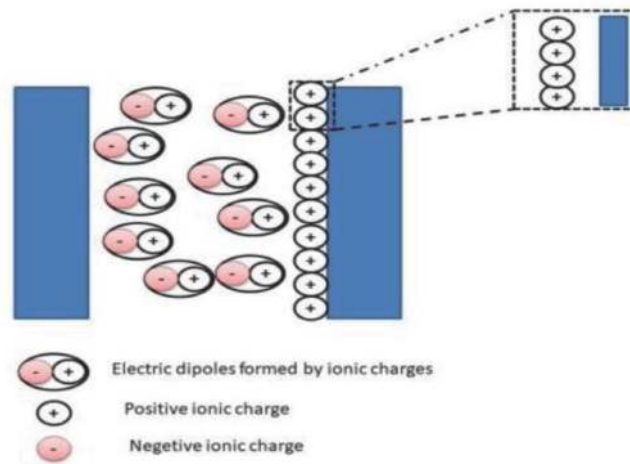
Electric dipoles formed by ionic charges

Positive ionic charge

Negetive ionic charge

Figure 7.
Schematic representation of the formation of the electric double layer in the matrix of polymer.

experimental analysis, however, depicted the capacitive effect of higher potentiality. On the basis of the physical model formerly manifested for the IPMC materials, it was noted that the capacitive effect was only corroborated with the formation of electric dipoles in between the positive ionic charges and fixed ionic charges those are located in between the double layer region and the positive electrode. In conclusion, there are two distinct capacitive effects: one is for the genesis of the double layer, and another is associated with the produced electric dipoles. To interpret for the two capacitive effects in the time frame of the voltage, an amendment was made to Eq. (6), containing the sum of a second exponential component linked with a second time constant, as Eq. (7) shows [52].

$$\vartheta\,(t) = a.e^{\frac{-t}{\tau 1}} + b.e^{\frac{-t}{\tau 2}} \tag{7}$$

The model now reflects two-time constants: a short time constant $\tau 1$ and a slow time constant $\tau 2$. The sum of those parameters a and b is equal to the IPMC voltage at the initial stage of the discharging methods. The capacitance value is obtained related with each time constant from Eqs (8) and (9). One of that time constants is associated with the capacitive effect in the IPMC linked with the electric dipole arrangement and which zone in the polymer resembles the region between the positive ionic charges and the fixed ionic charges. On the contrary, the second constant is allied with the double layer.

$$C1 = \frac{\tau 1}{Rext} \tag{8}$$

$$C2 = \frac{\tau 2}{Rext} \tag{9}$$

Using the revised model, a substantial enhancement was achieved, allowing assessing the value of capacitances C1 and C2 and the time constants connected with each type of IPMC system and for each type of electrolyte. The fact that the maximum capacitance was accomplished when using electrolytes with lower solute concentrations can be elucidated by the encapsulation effect [53]. The encapsulation effect ascends from the circumstance that the maximum number of electric dipoles designed in the polymer matrix is attained for a given solute concentration of the electrolyte. A definite limited number of electric dipoles will relate to a maximum yield of the dielectric constant of the IPMC matrix. Since the capacitance

concomitant with an IPMC is correlated to the dielectric constant using Eq. (9), it follows that the capacitance will incline to a maximum value at high solute concentrations. It should be recollected that $\tau 1$ is associated with the polymer region where the creation of electric dipoles in between positive ionic charges and fixed ionic charges happens and the region that will establish the characteristic times of charging and discharging of each IPMC system. However, an IPMC membrane having a higher thickness does not signify a greater time constant but directly proportional to the effective surface area. The difference in surface areas also delineates the alteration in results between the IPMC with the same thickness. Therefore, the second-largest surface area of the IPMC membrane in the research would be predictable to have higher yields than were acquired.

4.5 Discharge time

For an RC circuit, the load voltage during discharge of the capacitor over resistance is correctly given by Eq. (10).

$$\vartheta(t) = U0.e^{-\frac{t}{R.C}} \tag{10}$$

The discharging time constant τ is given by eqn

$$\tau = R.C \tag{11}$$

Replacing Eq. (11) into Eq. (9.20), one arises at the voltage at time t given by Eq. (12).

$$\vartheta(t) = \frac{U0}{e} \approx 0.368 Uo \tag{12}$$

The instantaneous at which the IPMC voltage reaches the value calculated by Eq. (12) is measured from all the experimental results. It was depicted that the majority of IPMC membranes offered results in the order of hundreds of seconds. Incrementing the values with enhancing electrolyte solute concentrations were also found. This system had the lowest surface area among the IPMC matrix analysed, thus having fewer electric dipoles along the electrodes of this matrix. The IPMC double-capacitance model undertakes two different capacitive effects; one is related with a fast time constant $\tau 1$ and with the other a slow time constant $\tau 2$. The significance of each time constants in the IPMC capacitor process is related to the frequency of the circuit in that it will be implanted. The capacitance C1 is leading in the case of high frequencies. Contrariwise, in low frequencies, the capacitance C2 will hold huge prominence in the operation of the IPMC capacitor. However, different functional features rely on the frequency operation of the circuit in which the IPMC is implanted; it is crucial to envisage its energy depending on the envisioned mode of operation. To calculate that percentage of the total stored energy can be free if high frequencies are used, the power degenerate in the resistive load in the time interval consistent to the first time constant—that is, from the initial time of the discharge until the time instant $\tau 1$—was calculated. Within these essays, two charging times importances had been taken care of analogous to two different time instants in the charging methods of the IPMC. The first time moment t corresponds to the instant at which the IPMC voltage value at its terminals is approximately 63% of the final value U, as shown in Eq. (13).

$$\vartheta(\tau) = U \left(1 - \frac{1}{e}\right) \approx 0.632 U \tag{13}$$

The second time instant is related to when the across IPMC terminals voltage equals 95% of its final value. These two moments were selected to depict the effect of the two-time constants of the system forecasted by the attuned electrical model. The best times were usually realised for higher solute concentrations, with the maximum having reached for IPMC using the higher electrolyte solute concentration. The charge time values are alike to the period of the cut-off frequency an IPMC element replies to mechanically. The charging time of an IPMC element is directly associated with its frequency response; meanwhile, this time interval resembles the time needed for much of the positive ionic charges stored inside the element is located on one of its electrodes, establishing dipole electric ionic in between positive and negative electric charges. Thus, one can authorise two charging time constants: a fast constant, which impacts the early charge stages, and a slow constant, with greater effect in the remaining moments. For cases of constant current charging, the model that expresses this fact is given by Eq. (14), where Umax is the IPMC voltage at the end of charging and the sum of the constants a and b is equal to 1.

$$\vartheta(\tau) = \text{Umax} \left(1 - ae^{\frac{-t}{\tau 1}} - be^{\frac{-t}{\tau 2}}\right) \tag{14}$$

4.6 Nominal voltage and number of charge: discharge cycle

To assess an IPMC matrix system's electric power density over the maximum energy stored for each IPMC, the rated voltage must know first. It has been contemplated that the nominal voltage of an IPMC polymer matrix to the extreme potential variance can happen at its terminals deprived of the electrolysis of the solvent. Electrolysis of water is a physical circumstance investigated by the water decomposition into its basic elements, namely oxygen molecules and hydrogen ions. This incident has the effect of concentration lowering of solvent present in the IPMC, reducing the ionic mobility within the IPMC. Moreover, the H+ ions formation enhances the density of positive ionic charges, leading to a temporary increment in the ionic current density. If an adequately high electric field is extended, the polymer matrix electro-active IPMC membrane material interruption may still happen, that instigating permanent destruction to the material. The target is to inspect the association between the number of charge–discharge cycles and the solute concentration of a given IPMC polymer matrix. Different IPMCs were evaluated rely on the electric energy originally stored in certain IPMCs equated with the values at the end of the limited number of charge–discharge cycles of the IPMC. It is noted that these results were also equated with all solute concentrations considered. The methodologies introduced to relate the stored energy at the initial and end of a test relates to the square of the voltage at IPMC terminals. After a particular time, the outcomes for the decrease in stored electric energy were calculated as a solute concentration function. When the IPMC system is charged up to a definite maximum voltage, and after a few seconds, the entire system allows for discharge typically without external influence, and the total charge dissipation has occurred consecutively. The entire time taken for discharge is fully its charge storing capabilities. The primary rapid decrement in the voltage is due to the downfall of the double layer shaped by the positive ionic charges and the electric ones on the electrodes. The electrical energy stored in a capacitive system is given by Eq. (15).

$$E = \frac{1}{2}.C.V^2 \tag{15}$$

In the time interval, the main incident was the reorganisation effect of the electric dipoles formed by ionic charges in the IPMC polymer matrix system.

As a result, the voltage at the IPMC lessened significantly. This voltage drop can be elucidated by evaporation of electrolyte, i.e., water in this case. However, the IPMC does not encapsulate; the evaporation of water will play a vital role in these circumstances [53]. As the solvent vaporises, this took away positive ionic charges, so the electric charge decreased within the IPMC system and the decreased number of electric dipoles. In some cases, it was observed that the membrane had dried, probably having some water in the matrix inside, which elucidates the presence of a residual voltage at its terminals. The energy density of stored electrical energy: It has been calculated that this type of capacitive element—the IPMC material possesses that is similar in nature to that of classic capacitors when used for energy storage. It is known, electrical energy is measured from the rated voltage and the capacitance. The power is proportional to the nominal voltage square directly, and, in turn, the rated voltage is proportional to the IPMC element thickness directly since the electrolysis of the solvent is catalysed by the electric field present within the IPMC system matrix. The energy density is exhibited by the ratio between the extreme energy the IPMC can store and its respective mass. It has also been seen that the response that incrementing the thickness of the IPMC does not impact energy density enhancement. This is a significant response that depicts that the price of a membrane of electro-active IPMC material becomes high prominently with the thickness. It is crucial to mention that the electrolyte a solution of salt and water for research purposes. If an electrolyte having a higher dielectric constant, like an electrolyte composed of lithium and propylene, had been introduced, it would be anticipated that the electric energy storage capacity of the IPMC materials matrix would be prominently enhanced. Lithium ions (Li^{2+}) developing the solute of the electrolyte has a lesser atomic radius than sodium ions (Na^+) and thus have higher ion transportation capabilities within a membrane of IPMC material, which accelerates the ion interaction between the sulfonate ions (SO^{3-}) and the positively charged ions attached to the polymer structure [54]. Moreover, this electrolyte's degree of evaporation is very low, which advances the preservation time of the electric charge of a capacitive IPMC material matrix.

5. Different applications of IPMC based energy harvesting and storage

5.1 Metal composites based ionic polymer on microcellular foamed Nafion

The energy harvesting experimentation of the IPMC composite membrane was lead in the 20 Hz frequency or less. When vibrations of a definite frequency window were allowed, the microcellular foamed samples were permitted, and a prominent proportion of energy was gathered from foamed samples compared to non-foamed samples. The outcome value was transformed by computing the modification data attained by the standardisation for the obtained current. In the band of frequency, the subsequent data was transformed into the value of root mean square (RMS), and also a 20 s time from the entire 30 min time approximately delineated the higher data was designated and connived. Two polymer membrane matrices were investigated in similar analysis environments, and the average value was accepted. For every analysis scenario, we connived a graphical output of current versus time. That was corroborated by that foamed IPMC samples logged a band of high frequency with the higher value. Moreover, in the band of low-frequency, it is depicted that the IPMC samples of non-foamed higher energy harvest compared to the foamed system. This analysis is accredited to the much critical non-foamed samples movements. In the band of frequency about 10 Hz, it was investigated that the foamed system deviate much higher swiftly than the
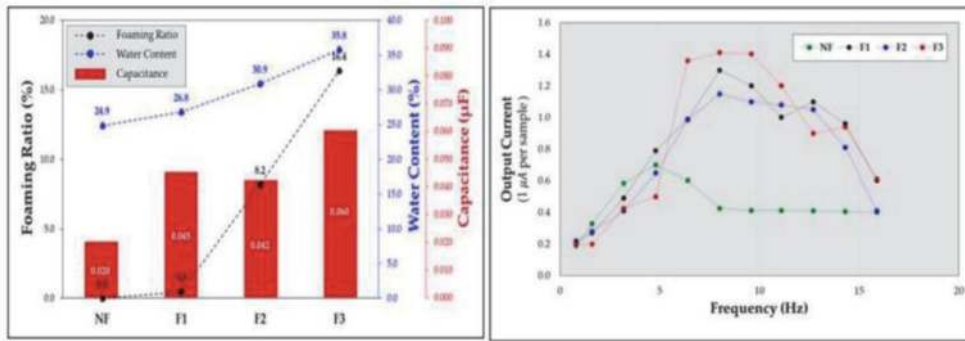
Figure 8.
Water content, capacitance, and output current versus frequency variations according to the foaming ratio of IPMC specimen [55].

specimen of non-foamed; also, the following data fluctuated up to roughly three times. The capacitance was calculated with the 0.001 µF resonance in the 120 Hz band after drying in a vacuum under all conditions of the specimen. Distinct outputs were gathered for every analysed system. As the ratio of foaming incremented, the retention capacity of cells' water was enhanced thereafter, along the capacitance was also incremented. It is presumed that the thickness increment in the membrane of polymer electrolyte and enhancement of water retentivity ameliorate the effective enactment of the capacitance. These are for the containing of water in the IPMC matrix and affecting the responses as a relaxation factor depicts the prominence outcome of the capacitance [55]. The obtained yields are delineated in **Figure 8**.

5.2 Ionic polymer-metal composite based water electrolysis for solar energy storage

The typical gas generation rate was calculated using the total volume of hydrogen gas composed divided by the duration of the 300 s. When the applied voltage increases, the gas generation rate enhances for all three IPMCs. Fascinatingly, the etched IPMC delineates a steeper increase compared to both the sanded and control IPMCs. Even though sanded and etched IPMC have higher whole gas production rates than the control IPMC, the sanded IPMC's gas generation rate was higher at a lower voltage, whereas the etched IPMC's gas generation rate was higher the higher voltage. To calculate the efficacy of the different fabrication process, the average gas production rate, the average voltage supplied, and the average current through the IPMC was computed to regulate the system's competence. From the graph, all three IPMC exhibits higher efficiency at lower voltage and their efficiency decrement at a variable rate as the voltage applied increases. Sanded IPMC has the highest efficiency and highest gas generation rate around 3 V, successfully producing that increasing the surface area through sanding will advance the performance of IPMC for energy harvesting. Although etching has a higher gas generation rate compared to the control, it must be noted that its energy efficiency values are often lower compared to both the sanded and control IPMC. On the other hand, at lower supply voltages, the electrolysers at higher temperatures were lagging in the generation of gas. However, the gas generation rate was higher at higher applied voltages, signifying a higher average slope in applied voltage vs. gas generation rate. The proficiency of the IPMC electrolyser generally decreases as the voltage applied increases. However, for higher temperatures (45°C, 55°C and 65°C), an increase in the productivity of the IPMC generator is seen as the voltage applied surges from 4 V to 5 V. When the temperature is low (45°C), it behaves similarly to IPMC at
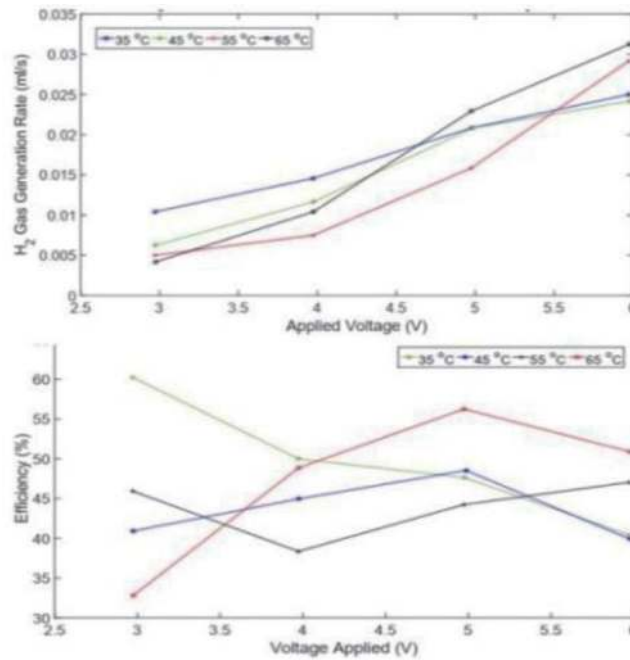
Figure 9.
Comparison illustration of IPMC H_2 production rate and IPMC electrolyser's efficiency under temperatures variation [56].

room temperature, however, when the temperature increases to 45°C, the electrolyser seems to hold a constant efficiency. As the temperature increases to 65°C, the efficiency seems to progress with increased voltage [56]. Comparison analysis illustrated in **Figure 9**.

5.3 Nafion-PVA composite membranes performance for direct methanol fuel cells

This research analysis has been targeted to investigate the permeability of methanol and fuel cell proficiency of Nafion-PVA composite membranes in the functionalities of the thickness in the range of 19 ∼ 97 μm. Also, the composite polymer membranes were fabricated by the Nafion polymer that is placed in the nanofibres of (PVA) polyvinyl alcohol. The methanol infusion resistance of the Nafion/PVA composite membranes exhibits a linear deviation versus thickness. The variation between actual and apparent permeability leads to a calculated data of 4.0×10–7 cm^2s^{-1} for the proper or intrinsic permeability in the phase-in bulk of the membranes in the composite matrix. The integration of nanofibers of PVA creates a noticeable decrease of one order scale in the permeability of methanol associated with Nafion original membranes. The proficiency of DMFC of the electrode membrane assemblages fabricated from pristine and Nafion-PVA membranes was analysed at 95°C, 70°C and, 45°C in different concentrations of methanol, like as 3, 2 or 1 M. The membranes polymer composite in nanoscale with the thicknesses of 47 μm and 19 μm corroborated densities of power of 184 $mWcm^{-2}$ and 211 $mWcm^{-2}$ in the temperature of 95°C and the concentration of 2 M methanol. It is analogous to the finding for membranes by Nafion with an analogous thickness of the similar conditions, 204 mW cm^{-2} and 210 mW cm^{-2}, correspondingly. However, a higher degree of utilisation of Nafion work as a material of proton-conductive in Nafion-PVA membranes is delineated for the lesser proportion of Nafion polymer in the membranes composite. Therefore, substantial reserves in the

expended Nafion amount are significantly achievable. Moreover, the PVA nanofibers incorporation in the time of fabrication exhibited the polymer membranes with lower thickness with higher mechanical attributes; however, the modification of membranes of pristine Nafion become unviable below the 50 μm thickness. The innovative membranes of nanocomposite are fabricated using Nafion polymer amalgamated in between the functionalised nanofibers of polyvinyl alcohol (PVA) and investigated the attribution of DMFC performance and methanol permeability. Furthermore, methanol's primary permeability is detected from the attribution of original permeability inherent to the material of the membrane matrix. The composite polymer membranes delineated the permeability coefficient of methanol with a magnitude reduction of one order compared to the pristine membrane of Nafion for the barrier effect triggered with the nanofibers. Furthermore, the nanofiber phase is not impacted in the coefficient of electro-osmotic drag of methanol; in some definite circumstances, the low values were detected in membranes of Nafion-PVA. Fascinatingly, the coefficient of electro-osmotic drag of methanol was decremented corresponding to temperature as an alternative of the water responses conveyed to increment with temperature increase. Direct methanol fuel cell analyses at variational methanol concentration and temperature conditions delineated the extreme outcomes to be attained in 2 M solutions at 95°C. In these scenarios, the membranes of Nafion-PVA of 47 and 19 μm of thickness attained comparable engagements to Nafion membranes with equivalent thickness compared to the high protonic resistance detected at the membranes polymer composite. Introducing a phase of nanofiber in the Nafion polymer matrix and the thin membranes use leading to important reserves in the expended Nafion polymer amount can be proficiently managed to keep higher performances [57].

5.4 Ocean-based energy production system using the electrochemical alteration of wave energy with the help of ionic polymer-metal composites

In this research work, ionic polymer with metal composites (IPMCs) based on an energy harvesting platform stored the kinetic energy from the waves of the ocean and transformed it into electricity. However, the investigational analysis depicted that IPMC composite materials attribute several benefits, like durability and softness; they also counter speedily to wave parameters like wavelength, amplitude, and frequency. Moreover, the data analysis recorded for 296-day delineated that the gross power density engendered persisted stability around 245 μW/m². The decaying electrical performance of IPMC polymer matrix in a span of long term process is trivial. Generally, the modules rotation is nominal: the 18 modules' gross amplitude in the motions of rolling, pitching, and yawing is roughly 1 degree in the 0.48 Hz frequency.

Furthermore, the displacement in the z-direction is profoundly high compared to the incident waves' amplitude and different displacements directions. The investigational outcomes demonstrated the gross power density intensely oscillated at a particular time in a day more than 180 μW/m², also with the power density average of roughly 245 μW/m² and 292 μW/m² peak value. The IPMC polymer system's power density is mostly smaller than the conventional energy resources; furthermore, the IPMC system is economical and sturdy. The system power can be enhanced by accumulating the effective area of the IPMC membrane matrix. On the other hand, several explorations will emphasise evaluating buoy systems in fluctuating wave and current presences to analyse the configuration system stability in the ocean at the time of extreme weather or typhoon. Those studies will assist in augmenting the long-term performance and lessening the prices of maintenance at

the installation time. Furthermore, the IPMC material bending plays a potential role to develop the proficiency of the energy harvesting structure [58].

5.5 Water and ion transportation in Perfluorosulfonated ionomer membranes for application of fuel cells

The volume fraction of water θ rises with lessening equivalent (EW) weight values of the IPMC membrane, irrespective of the membranes types and the counter cations. That point denotes the water present in the membranes matrix escalates with the concentration surges of the group of ion exchange. Afterwards, the water molecule presents in the groups of sulfonic acid and the counter cations within membranes to create the regions of the ionic cluster. On the other hand, anticipated that the membranes possess lesser EW values help to advance more numerous and much extensive ionic cluster zones in the membrane by providing high ionic conductivity. However, for the variation of cations species, the content of water order is $Na^+ < H^+ < Li^+$ for all the matrix of membranes. It designates that the content of water relies on the species of cations, and specifically, Li + cations can fetch the molecules of water for having the higher hydrophilic features. The ion-exchange group contributes to the formation regions of the ionic cluster. The total water molecules number in the membrane per ion-exchange group is λ also enhances with lessening the equivalent weight value; also, the order of λ for cations species variation is similar with the volume fraction of water $Na^+ < H^+ < Li^+$. It is advised that the number and size of regions of a cluster of ions in the matrix of membranes are pressurising with the value of the equivalent weight and the cations species variation. This signifies that when the equivalent weight diminishes, the counter cations and groups of sulfonic acid attract much water in the ionic ambience. The content of water is calculated by the stability in between the force of osmotic hydration in the ion and elastic force cluster persuaded with the fluorinated polymer deformation that is the leading chain. The activity of water can be equally presumed in the membrane matrix and the outer side of the solution of the membrane.31 If the number and size of the cluster region of ions enhance by escalating the membrane volume, the membranes density will be diminished for the water thickness (ca. at 25°C 1 g cm-3,) is lesser than the membranes itself (at 25°C around 2 g cm-3). The membrane densities reduce with reducing the equivalent weight value, particularly the Li-form membranes thicknesses that are lesser than the different cations-form membranes.

Furthermore, the membrane possesses a lesser equivalent weight value that enlarges the volume, and the cluster regions of ion are primarily developed mostly, specifically in the membrane of Li-form. The membrane possesses a lesser equivalent weight value that can create greater expanded cluster regions of ions despite the cations' species. The membranes' ionic conductivity is roughly correlated with the number and the size of cluster regions of ions in the matrix of membranes. Furthermore, the conductivity of all protonic membranes is significantly greater than the rest of the membranes of cationic form. It is usually attributed that the proton of the aqueous solution is elated with the help of the hopping process and can be transported faster compared to the rest of the cationic species transferred using the vehicle process. The probable aspects of finding out the conductivity are the mobility and concentration of carrier cations within the matrix of membranes that is calculated from the outcomes of the density of membrane and conductivity of ions. The sulfonic acid group concentration within the membranes, i.e. C_{SO3-} is analysed and equivalent to the carrier cations attention. However, the carrier cations concentration for all membranes is impervious to the equivalent weight value of membranes. The carrier cations species mobility is enhanced with reducing the

EW value. Like this, the increment of carrier cations mobility becomes an initial factor in enhancing the membranes conductivity. Moreover, the perfluoro sulfonate ionomers are not membranes of the cross-linked polymer. The EW value decrease leads to increasing the cations species number and expanding the membrane volume for the swelling.

The motion of water molecules in the polymer membranes is subjective with electrostatic counteraction by the cationic species; the water molecules mobility within membranes are diminished when the stronger interaction is present, and the membrane's diffusion rate will be slower with the reduction of water molecules. Furthermore, the cations species and water molecules' mobility in the polymer membranes is prominently crucial to comprehend the ionic movement in the membranes. In this scenario, the coefficient of water transmission tH$_2$O and the permeability of water Lp are significant parameters; they also provide such particulars about transportation. One carrier cation dragged that much water molecules denoted tH$_2$O holds a positive charge when cation transports within membranes. If this value becomes higher, the molecules of water intermingle with the cation species to the membranes more sturdily.

On the other hand, Lp depicted that the rate of permeation of water molecules within membranes. The diffusion of water molecules arises more smoothly in the membranes when the value is higher. The tH2O value of the Na$^+$ and Li$^+$ form membranes depicted high values compared to the membranes of the H-form. The Lp Na-form and Li$^+$ membranes are lesser than the membranes of the H-form. The Na$^+$ and Li$^+$ cations have sturdier counteractions compared to protons in the membranes with water molecules and avoid the diffusion of water molecules.

Moreover, the yield results delineated of the H-form membranes is the transportation of proton controlled by the hopping process, and the molecules of water are dragged hardly together at the time of proton transportation within membranes. In this case, the water molecules easily diffuse compared to Na-and Li-form membranes. The variation in Lp and tH$_2$O with respect to the EW value exhibits importance for water molecules with ion transport. The tH$_2$O is not systematically varied in the proton membranes, with the increment of Lp with EW value decrement. The two distinct parameters, water permeability and water transference coefficient, have better associations with the membranes conductivity. It is corroborated that the water molecules move more easily, in which membrane depicted higher ionic conductivity. The water molecules mobility within membranes correlated with the conductivity and is motivated by the cation species and the equivalent weight value. To envisage the interrelation between the cation species and the water mobility in elaborate, the analysis of the coefficients of self-diffusion DLi$^+$ and DH$_2$O was calculated by Li, and 1H PGSE-NMR are investigated. The values of DH$_2$O are about 10^{-10} m^{2}s^{-1} in the membranes. The acquired value for the proton Nafion 117 is very similar as investigated by Zawodzinski et al. in the temperature of 30°C. It is identified that the DH$_2$O value of pure H$_2$O at 30°C is 2.55×10^{-9} m^{2}s^{-1}. So the molecules of water mobility in the membranes are decreased. The DH$_2$O of the membranes enhances with reducing the EW value. The H-form membranes depict high values compared to the Na- and Li-form membranes. Those obtained outputs indicate that the water molecules transportation within membranes is decreased with the channel morphology of the cluster of ion zones and the interactivity by the species of a cation. Moreover, the molecules of water penetrate more rapidly in the Nafion membranes compared to the flemion membranes in the almost equivalent EW value. Also, it is fascinating that the polymer matrix membrane morphology impacts the membranes' conductivity. As a carrier ion, the movement of Li$^+$ is much connected to the water molecules transports in the membrane matrix. This is illustrated in **Figure 10**, here DLi$^+$ is illustrated versus DH$_2$O of the similar
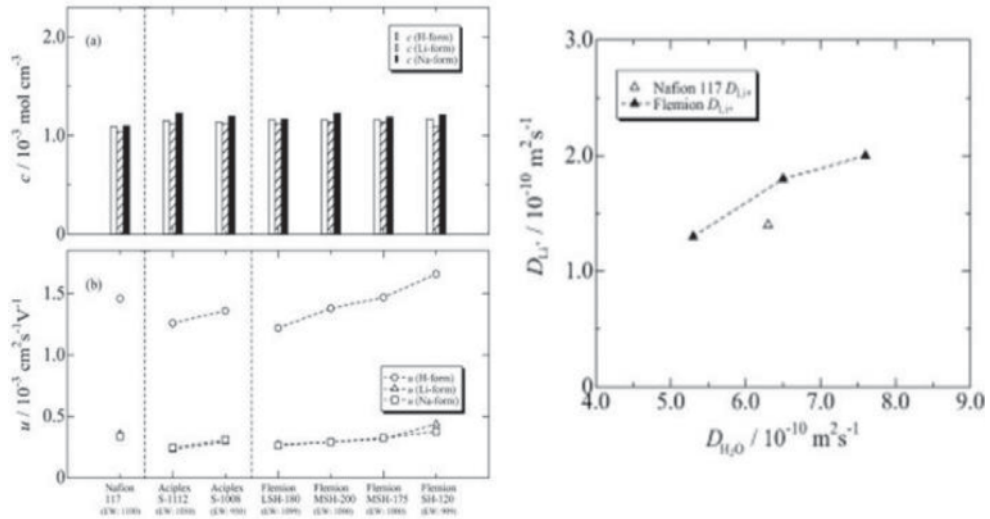
Figure 10.
Mobility u and *concentration* c *of carrier cations species in dissimilar membranes at the wholly hydrated state and the illustration of coefficient of self-diffusion of Li^+ cation* D_{Li}^+ *within Li-form membranes versus water molecule* D_{H2O} *[59]*.

membranes. Generally, the diffusion phenomenon (small-range) is quicker than diffusion of longer-range is elucidated as inconsistent diffusion.

Moreover, the time-dependent DH_2O illustrates that the molecules of water disperse in the heterogeneous region in the membranes. The areas of an ionic cluster are not the open area for the H_2O diffusion, and the interaction of water molecules with SO^{3-} and Li^+ shows dissimilar exchange rates. All of the obtained coefficients of self-diffusion analyses for Li^+ cation and water molecule by the PGSE NMR procedure are correlated well with other investigations of ionic conductivity, water content, water permeability, and water transference coefficient. Moreover, it is becoming a potential tool to comprehend water and ion-molecule transportation performance within the membranes [58].

6. Conclusion

This chapter represented the energy storage application with results and the practical characteristics of IPMC polymer materials in the analogous field. This composite polymer and polymer matrix have been researched in detail in the potential application of flexible energy storage of electrical energy. The attributes create the IPMC polymer materials prominent and potential elements for substituting the conventional capacitors in different real-time applications. These whole chapter goals delineate the summary of IPMC polymer material on energy storage and its corresponding working principles. There is plenty of fabrication methods comprising the primary process of compositing membrane and electrode of membrane surface discussed in detail. The coefficient of electro-osmotic drag of methanol is varied with temperature directly proportional. Direct methanol fuel cells analysed at different temperatures and methanol concentration delineated the highest performances in 2 M solutions at 95°C. The Nafion-PVA membranes of 47 μm and 19 μm thickness depicted proficient response, though the protonic resistance is high of composite membranes. The Nafion film thickness is enhanced the electrical harvesting response considering the more water retention in its internal pores. The foaming ratio escalation modifies the structure internally of

electrolyte membrane and enhances the harvesting phenomena, and that corroborated to increase storage of electric charge and modification of capacitance, with augmentation of water. The content of water in the membranes depicted the propensity of the increment of ionic cluster areas number with size though equivalent weight value decreased and the Li + form membranes fashioned the biggest regions of the ionic cluster. Also, the coefficients of water transfer and permeability denoted that in the Na- and Li-form membranes, the interaction of water molecules much sturdily with cations compared to proton when it can transport within membranes, and the molecule of water diffusion is decreased. The research analysis illustrated that surface area increment of IPMC by the etching and surface sanding enhances the gas generation rate of the IPMC electrolyser. The temperature increment of water effect on the IPMC electrolyser and the analysis data depicts the sharp enhancement of gas generation rate with the voltage applied to the generator ameliorates. Generally, the module's rotation is very less along with the gross amplitude of the 18 modules in the yaw, rolling and pitching motions is roughly 1 degree at 0.48 Hz. Moreover, the displacement in the z-direction is substantially high compared to the incident wave's amplitude and displacements of other directions. The experimental analysis delineated that gross power density at a particular time of a day sturdily fluctuated above 180 $\mu W/m^2$, along with power density of roughly 245 $\mu W/m^2$ with 292 $\mu W/m^2$ peak value. This polymer matrix system and its prominence application in electrical energy storage are yet to investigate more, and there are lots of parts that have to be explored in upcoming times. This chapter will also be beneficial in comprehending the IPMC polymeric matrix system to plenty of interested researchers in electro-active polymers. To be precise, the application of IPMC materials in electrical energy storage acts as guidance.

Acknowledgements

Author details

Monojit Mondal, Arkaprava Datta and Tarun Kanti Bhattacharyya*
School of Nanoscience and Technology, IIT Kharagpur, Kharagpur, W.B., India

*Address all correspondence to: tkb@ece.iitkgp.ac.in

IntechOpen

References

[1] Bandopadhya, Dibakar, and James Njuguna. "Estimation of bending resistance of ionic polymer metal composite (IPMC) actuator following variable parameters pseudo-rigid body model." *Materials Letters* 63, no. 9-10 (2009): 745-747.

[2] Brunetto, Paola, Luigi Fortuna, Salvatore Graziani, and Salvatore Strazzeri. "A model of ionic polymer–metal composite actuators in underwater operations." *Smart materials and Structures* 17, no. 2 (2008): 025029.

[3] Santos, J., B. Lopes, and PJ Costa Branco. "Ionic polymer–metal composite material as a diaphragm for micropump devices." *Sensors and Actuators A: Physical* 161, no. 1-2 (2010): 225-233.

[4] Tadokoro, Satoshi, Shinji Yamagami, Toshi Takamori, and Keisuke Oguro. "An actuator model of ICPF for robotic applications on the basis of physicochemical hypotheses." In *Proceedings 2000 ICRA. Millennium Conference. IEEE International Conference on Robotics and Automation. Symposia Proceedings (Cat. No. 00CH37065)*, vol. 2, pp. 1340-1346. IEEE, 2000.

[5] Wang, Xuan-Lun, Il-Kwon Oh, Jun Lu, Jinhun Ju, and Sunwoo Lee. "Biomimetic electro-active polymer based on sulfonated poly (styrene-b-ethylene-co-butylene-b-styrene)." *Materials Letters* 61, no. 29 (2007): 5117-5120.

[6] Keawboonchuay, C., and T. G. Engel. "Maximum power generation in a piezoelectric pulse generator." *IEEE transactions on plasma science* 31, no. 1 (2003): 123-128.

[7] Xu, Chao-Nan, Morito Akiyama, Kazuhiro Nonaka, and Tadahiko Watanabe. "Electrical power generation characteristics of PZT piezoelectric ceramics." *IEEE transactions on ultrasonics, ferroelectrics, and frequency control* 45, no. 4 (1998): 1065-1070.

[8] Mondal, Monojit, Dipak Kumar Goswami, and Tarun Kanti Bhattacharyya. "Lignocellulose based Bio-waste Materials derived Activated Porous Carbon as Superior Electrode Materials for High-Performance Supercapacitor." *Journal of Energy Storage* 34 (2021): 102229.

[9] Mondal, Monojit, Dipak Kumar Goswami, and Tarun Kanti Bhattacharyya. "Solvent dependent fabrication of Manganese Vanadium Oxide as cathode material for high performing supercapacitor." In *2020 4th International Conference on Electronics, Materials Engineering & Nano-Technology (IEMENTech)*, pp. 1-6. IEEE, 2020.

[10] Mondal, Monojit, Dipak Kumar Goswami, and Tarun Kanti Bhattacharyya. "Microwave synthesized manganese vanadium oxide: High performing electrode material for energy storage." *Materials Today: Proceedings* (2021).

[11] Mondal, M., B. Das, P. Howli, N. S. Das, and K. K. Chattopadhyay. "Porosity-tuned NiO nanoflakes: Effect of calcination temperature for high performing supercapacitor application." *Journal of Electroanalytical Chemistry* 813 (2018): 116-126.

[12] Bar-Cohen, Yoseph, and Qiming Zhang. "Electro-active polymer actuators and sensors." *MRS bulletin* 33, no. 3 (2008): 173-181.

[13] Bar-Cohen, Yoseph. "Electro-active Polymer (EAP) Actuators as Artificial Muscles: Reality." *Potential, and Challenges (SPIE-The International Society for Optical Engineering, Bellingham, Washington, 2001)* (2004).

[14] Oguro, K. "Bending of an ion-conducting polymer film-electrode composite by an electric stimulus at low voltage." *J. Micromachine Society* 5 (1992): 27-30.

[15] Sadeghipour, K., R. Salomon, and S. Neogi. "Development of a novel electrochemically active membrane and'smart'material based vibration sensor/damper." *Smart Materials and Structures* 1, no. 2 (1992): 172.

[16] Grodzinsky, Alan Jay. "Electromechanics of deformable polyelectrolyte membranes." PhD diss., Massachusetts Institute of Technology, 1974.

[17] Kim, Seong Jun, In Taek Lee, and Yong Hyup Kim. "Performance enhancement of IPMC actuator by plasma surface treatment." *Smart materials and structures* 16, no. 1 (2007): N6.

[18] Nemat-Nasser, Sia, and Jiang Yu Li. "Electromechanical response of ionic polymer-metal composites." *Journal of Applied Physics* 87, no. 7 (2000): 3321-3331.

[19] Peng, Jing, and Thomas A. Zawodzinski. "Describing ion exchange membrane-electrolyte interactions for high electrolyte concentrations used in electrochemical reactors." Journal of Membrane Science 593 (2020): 117340.

[20] Yu, Min., Shen, Hui., Dai, Zhen-dong., "Manufacture and Performance of Ionic Polymer-Metal Composites," Journal of Bionic Engineering, Vol. 4, No. 3, pp. 143−149, 2007

[21] Lee, S. J., Han, M. J., Kim, S. J., Jho, J. Y., Lee, H. Y. and Kim, Y. H., "A new fabrication method for IPMC actuators and application to artificial fingers," Smart Mater. Struct., Vol.15, No. 5, pp. 1217-1224, 2006.

[22] Kim, B. K., Kim, B. M., Ryu, J. W., Oh, I.-H., Lee, S.-K., Cha, S.-E. and Pak,

J. H., "Analysis of mechanical characteristics of the ionic polymer metal composite (IPMC) actuator using cast ion-exchange film," Proc. of SPIE, Vol. 5051, pp. 486-495, 2003.

[23] Jung SY, Ko SY, Park J-O, "Park S. Enhanced ionic polymer–metal composite actuator with pore size–controlled porous Nafion membrane using silica sol–gel process," Journal of Intelligent Material Systems and Structures, Vol. 28(11), pp. 1514-1523, 2017.

[24] Ijeri, Vijaykumar., Cappelletto, Lucandrea., Bianco, Stefano., Tortello, Mauro., Spinelli, Paolo., Elena, Tresso., "Nafion and carbon nanotube nanocomposites for mixed proton and electron conduction," Journal of Membrane Science - J MEMBRANE SCI, Vol. 363, pp. 265-270, 2010

[25] Chung, C. K., Fung, P. K., Hong, Y. Z., Ju, M. S., Lin, C. C. K. and Wu, T. C., "A novel fabrication of ionic polymer-metal composites (IPMC) actuator with silver nanopowders," Sens. Actuators B: Chemical, Vol. 117, No. 2, pp. 367-375, 2006.

[26] Shahinpoor, M., "Ionic polymer-conductor composites as biomimetic sensors, robotic actuators and artificial muscles: a review," Electrochim. Acta, Vol. 48, No. 14-16, pp. 2343-2353, 2003.

[27] Bhandari, Binayak, Gil-Yong Lee, and Sung-Hoon Ahn. "A review on IPMC material as actuators and sensors: fabrications, characteristics and applications." *International journal of precision engineering and manufacturing* 13, no. 1 (2012): 141-163

[28] Kim, Kwang J., and Mohsen Shahinpoor. "Ionic polymer–metal composites: II. Manufacturing techniques." *Smart materials and structures* 12, no. 1 (2003): 65.

[29] Millet, P., M. Pineri, and R. Durand. "New solid polymer electrolyte

composites for water electrolysis." *Journal of Applied Electrochemistry* 19, no. 2 (1989): 162-166.

[30] Brufau-Penella, J., M. Puig-Vidal, P. Giannone, S. Graziani, and S. Strazzeri. "Characterization of the harvesting capabilities of an ionic polymer metal composite device." *Smart materials and structures* 17, no. 1 (2007): 015009.

[31] Onishi, Kazuo, Shingo Sewa, Kinji Asaka, Naoko Fujiwara, and Keisuke Oguro. "Bending response of polymer electrolyte actuator." In *Smart Structures and Materials 2000: Electroactive Polymer Actuators and Devices (EAPAD)*, vol. 3987, pp. 121-128. International Society for Optics and Photonics, 2000.

[32] Shahinpoor, Mohsen, and Kwang J. Kim. "The effect of surface-electrode resistance on the performance of ionic polymer-metal composite (IPMC) artificial muscles." *Smart Materials and Structures* 9, no. 4 (2000): 543.

[33] Shahinpoor, Mohsen. "Ionic polymer–conductor composites as biomimetic sensors, robotic actuators and artificial muscles—a review." *Electrochimica Acta* 48, no. 14-16 (2003): 2343-2353.

[34] De Gennes, P. G., Ko Okumura, M. Shahinpoor, and Kwang J. Kim. "Mechanoelectric effects in ionic gels." *EPL (Europhysics Letters)* 50, no. 4 (2000): 513.

[35] Kim, Kwang J., and Mohsen Shahinpoor. "Ionic polymer–metal composites: II. Manufacturing techniques." *Smart materials and structures* 12, no. 1 (2003): 65.

[36] Anand, S. V., K. Arvind, P. Bharath, and D. Roy Mahapatra. "Energy harvesting using ionic electro-active polymer thin films with Ag-based electrodes." *Smart Materials and Structures* 19, no. 4 (2010): 045026.

[37] Griffiths, David John. "Development of ionic polymer metallic composites as Sensors." PhD diss., Virginia Tech, 2008.

[38] Shahinpoor, Mohsen, and Kwang J. Kim. "Ionic polymer–metal composites: IV. Industrial and medical applications." *Smart materials and structures* 14, no. 1 (2004): 197.

[39] Peng, Wuxian, Yajing Zhang, Jinhai Gao, Yiming Wang, Yang Chen, and Yiran Zhou. "Fabrication and performance of ionic polymer-metal composites for biomimetic applications." *Sensors and Actuators A: Physical* 299 (2019): 111613.

[40] Bonomo, Claudia, Luigi Fortuna, Pietro Giannone, and Salvatore Graziani. "A sensor-actuator integrated system based on IPMCs [ionic polymer metal composites]." In *SENSORS, 2004 IEEE*, pp. 489-492. IEEE, 2004.

[41] Martin, Benjamin Ryan. "Energy harvesting applications of ionic polymers." PhD diss., Virginia Tech, 2005.

[42] Pandolfo, Anthony G., and Anthony F. Hollenkamp. "Carbon properties and their role in supercapacitors." *Journal of power sources* 157, no. 1 (2006): 11-27.

[43] Yeo, R. S., J. McBreen, G. Kissel, F. Kulesa, and S. Srinivasan. "Perfluorosulphonic acid (Nafion) membrane as a separator for an advanced alkaline water electrolyzer." *Journal of Applied Electrochemistry* 10, no. 6 (1980): 741-747.

[44] Conte, Mario. "Supercapacitors technical requirements for new applications." *Fuel cells* 10, no. 5 (2010): 806-818.

[45] Kaempgen, Martti, Candace K. Chan, J. Ma, Yi Cui, and George Gruner. "Printable thin film supercapacitors using single-walled carbon nanotubes." *Nano letters* 9, no. 5 (2009): 1872-1876.

[46] Kularatna, Nihal, Jayathu Fernando, Amit Pandey, and Sisira James. "Surge capability testing of supercapacitor families using a lightning surge simulator." *IEEE transactions on Industrial Electronics* 58, no. 10 (2011): 4942-4949.

[47] Landrock, Clinton K., and Bozena Kaminska. "Ionomer composite thin film capacitors." *IEEE Transactions on Components, Packaging and Manufacturing Technology* 1, no. 9 (2011): 1305-1310.

[48] Chuo, Yindar, Clint Landrock, Badr Omrane, Jeydmer Aristizabal, Jasbir N. Patel, Marcin Marzencki, and Bozena Kaminska. "Towards self-powering touch/flex-sensitive OLED systems." *IEEE Sensors Journal* 11, no. 11 (2011): 2771-2779.

[49] Branco, PJ Costa, and J. A. Dente. "Derivation of a continuum model and its electric equivalent-circuit representation for ionic polymer–metal composite (IPMC) electromechanics." *Smart Materials and Structures* 15, no. 2 (2006): 378.

[50] Invernizzi, Costante Mario. "Prospects of mixtures as working fluids in real-gas Brayton cycles." *Energies* 10, no. 10 (2017): 1649.

[51] Shahinpoor, Mohsen, ed. *Ionic Polymer Metal Composites (IPMCs): Smart Multi-Functional Materials and Artificial Muscles, Volume 2*. Royal Society of Chemistry, 2015.

[52] Robinson, Walter Junkin. "Charge control of ionic polymers." PhD diss., Virginia Tech, 2005.

[53] Kokya, Bahman Ahmadzadeh, and Taher Ahmadzadeh Kokya. "Proposing a formula for evaporation measurement from salt water resources." *Hydrological Processes: An International Journal* 22, no. 12 (2008): 2005-2012.

[54] Santos, J., B. Lopes, and PJ Costa Branco. "Ionic polymer–metal composite material as a diaphragm for micropump devices." *Sensors and Actuators A: Physical* 161, no. 1-2 (2010): 225-233

[55] Kweon, Byung Chul, Joo Seong Sohn, Youngjae Ryu, and Sung Woon Cha. "Energy Harvesting of Ionic Polymer-Metal Composites Based on Microcellular Foamed Nafion in Aqueous Environment." In Actuators, vol. 9, no. 3, p. 71. Multidisciplinary Digital Publishing Institute, 2020

[56] Keow, Alicia, and Zheng Chen. "A study of water electrolysis using ionic polymer-metal composite for solar energy storage." In *Smart Materials and Nondestructive Evaluation for Energy Systems 2017*, vol. 10171, p. 1017104. International Society for Optics and Photonics, 2017

[57] Mollá, Sergio, and Vicente Compañ. "Performance of composite Nafion/PVA membranes for direct methanol fuel cells." *Journal of Power Sources* 196, no. 5 (2011): 2699-2708.

[58] Vinh, Nguyen Duy, and Hyung-Man Kim. "Ocean-based electricity generating system utilizing the electrochemical conversion of wave energy by ionic polymer-metal composites." Electrochemistry Communications 75 (2017): 64-68.

[59] Saito, Morihiro, Naoko Arimura, Kikuko Hayamizu, and Tatsuhiro Okada. "Mechanisms of ion and water transport in perfluorosulfonated ionomer membranes for fuel cells." The Journal of Physical Chemistry B 108, no. 41 (2004): 16064-16070.